

## DISPERSIVE OPTICAL CONSTANTS OF THERMALLY EVAPORATED $\text{Se}_{70-x}\text{Te}_{30}\text{Pb}_x$ THIN FILMS

K. MALIK\*, PARVINDER, A. GUPTA, P. KUMAR

*Material Science Research Laboratory, Department of Physics, Gurukula Kangri University, Haridwar 249404, India.*

Thin films of amorphous  $\text{Se}_{70-x}\text{Te}_{30}\text{Pb}_x$  ( $x= 0, 2, 4, 6$  and  $8$ ) are deposited on glass substrate by thermal evaporation technique. Transmittance measurements were used to calculate refractive index  $n$  and the extinction coefficient  $k$  using Swanepole's method. The oscillator energy  $E_0$ , dispersion energy  $E_d$ , and other parameters have been determined by Wemple - DiDomenico single oscillator approach. The optical band gap  $E_g$  is estimated using Tauc's relation and is found to decrease with the increasing Pb content. The decrease in optical band gap is interpreted in terms of electronegativity difference of constituent atoms and average bond energy difference of the system.

(Received January 20, 2015; Accepted March 6, 2015)

*Keywords:* Refractive index, Oscillator energy, Dispersion energy, Optical band gap.

### 1. Introduction

Chalcogenide glasses are also called lone-pair semiconductors, because the conduction properties determines by the lone-pair band [1]. These glassy materials have received great attention because of their important optical applications in the infrared region due to their high optical transparency in IR region [2]. In the amorphous state, Se- rich chalcogenide glasses drew great attention and were subjected to a lot of investigation due to their high glass forming ability. In pure state Se has several disadvantage because of its short life time and low sensitivity. The impurity like Te, Ge, Sb, Sn, Bi and Pb etc. are used to prepare alloys with Se which are more sensitive, having greater hardness, small aging effect and higher crystallization temperature. The Se-Te alloys have been found to be more useful from the technological point of view due to their greater hardness, higher  $T_c$ , and lower ageing effect as compared to amorphous Se [3, 4]. Besides, the physical properties of these glassy alloys are strongly dependent on their compositions.

The optical properties of chalcogenide thin films have been the subject of numerous studies due to their technological importance. In the present system, we have used Se as a major content because it is widely used as a typical glass former. Here we have chosen Te as an additive to Se. The aim of present paper is to study the effect of Pb incorporation, at the expense of Se content, on the optical properties of as prepared  $\text{Se}_{70-x}\text{Te}_{30}\text{Pb}_x$  (where  $x= 0, 2, 4, 6$  and  $8$ ) thin films. The addition of third element Pb in Se-Te alloys expands the glass forming region and it is also expected that it brought a change in the structural and optical parameters of Se-Te alloys. The present work deals with the determination of the optical band gap, refractive index, extinction coefficient, real & imaginary dielectric constants of Se-Te-Pb thin films by analyzing the transmission spectra in the 700- 1800 nm wavelength range.

### 2. Experimental details

Different compositions of bulk  $\text{Se}_{70-x}\text{Te}_{30}\text{Pb}_x$  ( $x= 0, 2, 4, 6$  and  $8$ ) chalcogenide glasses were prepared by melt quenching technique. Highly pure (99.999 %) Se, Te, & Pb elements (Alfa

---

\* Corresponding author: kapilmalik08@gmail.com

Aesar U.S.A.), were weighted according to their atomic weight percentages. The material was then sealed in evacuated ( $10^{-5}$  Torr) quartz ampoule (length  $\sim 6$  cm and internal diameter  $\sim 8$  mm). The sealed ampoules containing materials were kept inside a vertical muffle furnace whose temperature was raised at a rate of 3 K/minute up to  $950^{\circ}\text{C}$  for 24 hours. During heating, the ampoules were constantly rocked, by rotating a stainless steel rod to which the ampoules was tucked away in the furnace, to ensure the homogenization of the melt. After rocking for about 24 hours, the obtained melt was rapidly quenched in ice cooled water. The ingots of quenched samples were taken out by breaking the quartz ampoules.

The chalcogenide thin films used in the present study of the system were deposited by thermal evaporation technique on to glass substrates at base pressure of  $\approx 4 \times 10^{-6}$  mbar using a HINDHIVAC coating unit (Model No. 12A4D). Prior to thin films deposition the substrates were carefully cleaned. Commercially available glass slides (Blue Star, Mumbai, India) are dipped in chromic acid for three hours, then washed with liquid detergent and finally ultrasonically cleaned with acetone [8].

During vacuum deposition, the temperature of the substrate was maintained at room temperature (300 K) to avoid re-evaporation of any condensed component. During the deposition process the substrate holder was also rotating at a speed of  $\approx 50$  rpm, which makes it possible to obtain film of uniform thickness [9]. The deposition rate was  $\approx 1-5 \text{ \AA S}^{-1}$ , and it was continuously measured by a quartz crystal monitor. This low deposition rate results in the composition of the thin film is very close to the composition of the starting material [10]. The films were kept inside the deposition chamber for 24 h to attain thermodynamic equilibrium as suggested by Abkowitz [11].

XRD studies were carried out to get an idea about the nature of as deposited thin films. A model no. Xpert - Pro MPD, X-ray diffractometer was employed for studying the structure of the prepared material in thin film form. The copper target was used as a source of x-rays with  $\lambda = 1.5404 \text{ \AA}$  ( $\text{Cu K}\alpha_1$ ). The scanning angle was in the range of 5- 65 Degree.

For all the samples, the optical transmission spectra were recorded at normal incidence of light, in the wavelength range 700- 1800 nm, by using a double beam (Shimadzu UV 3600) spectrophotometer. The spectrophotometer was set with a suitable slit width of 1 nm in the measured spectral range. All measurements were obtained at room temperature (300 K). The measured transmittance spectra were used to calculate the optical constants and optical band gap ( $E_g$ ) for the different compositions of  $\text{Se}_{70-x}\text{Te}_{30}\text{Pb}_x$  thin films with a glass substrate in the reference beam.

### 3. Results and discussion

#### 3.1 X-ray diffraction pattern

Fig. 1 shows the X-ray diffraction patterns for all as deposited films. The XRD pattern of  $\text{Se}_{70-x}\text{Te}_{30}\text{Pb}_x$  ( $x=0, 2, 4, 6$  and  $8$ ) films show no sharp peaks which confirms the glassy nature of as deposited thin films.

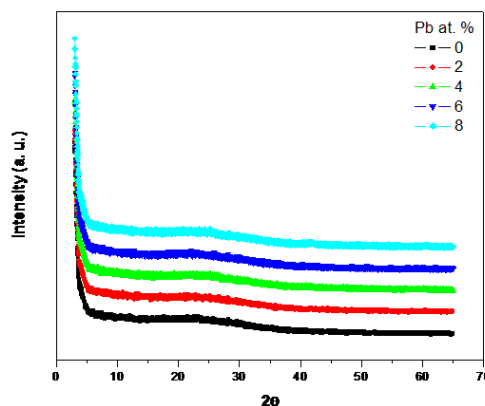


Fig. 1. X-ray diffraction pattern of as deposited  $\text{Se}_{70-x}\text{Te}_{30}\text{Pb}_x$  films.

### 3.2 Optical properties

For all the prepared thin film samples, optical transmission was measured in the wavelength range 700–1800 nm. The optical constants are obtained by using only the transmission spectrum. The optical parameters are calculated by using Swanepoel's method [12, 13], which is based on the approach of Manifacier et. al. [14].

#### 3.2.1 Determination of optical constants

For the method proposed by Swanepoel [12, 13], the optical constants are deduced from the fringe patterns in the transmittance spectrum. The refractive index in the transmittance region where  $\alpha \approx 0$  was calculated by using the formula.

$$n = \sqrt{N + \sqrt{N^2 - s^2}} \quad (1)$$

where

$$N = \frac{2s}{T_{min}} - \frac{(s^2 + 1)}{2} \quad (2)$$

In the weak region where the absorption coefficient ( $\alpha \neq 0$ ) the value of N is given by

$$N = 2s \frac{T_{max} - T_{min}}{T_{max}T_{min}} + \frac{s^2 + 1}{2} \quad (3)$$

where  $T_{max}$  is the upper extreme transmission point and  $T_{min}$  lower extreme transmission point for particular wavelength and 's' is the refractive index of the glass substrate ( $s=1.52$ ).

If  $n_1$  and  $n_2$  are the refractive indices of two adjacent maxima or minima at wavelengths  $\lambda_1$  and  $\lambda_2$ , then the thickness of the film is given by

$$d = \frac{\lambda_1 \lambda_2}{2(\lambda_1 n_2 - \lambda_2 n_1)} \quad (4)$$

The extinction coefficient k can be calculated from the following relation

$$k = \frac{\lambda}{4\pi d} \ln\left(\frac{1}{x}\right) \quad (5)$$

Where  $x$  is the absorbance, given by

$$x = \frac{E_M - \sqrt{E_M^2 - (n^2 - 1)^3(n^2 - s^4)}}{(n - 1)^3(n - s^2)} \quad (6)$$

and

$$E_M = \frac{8n^2s}{T_{max}} + (n^2 - 1)(n^2 - s^2) \quad (7)$$

The absorption coefficient  $\alpha$  can be calculated from the relation given as

$$\alpha = \frac{4\pi k}{\lambda} \quad (8)$$

The variation of transmission (T) with wavelength ( $\lambda$ ) for amorphous  $\text{Se}_{70-x}\text{Te}_{30}\text{Pb}_x$  thin films is shown in fig. 2. The spectrum shows fringes due to interference at various wavelengths. The non-shrinking interference fringe pattern indicates for homogeneity of the deposited films.

The maxima and minima of these fringes are used to calculate the various optical constants. It was found that maxima and minima of the fringes shift towards higher wavelength side as the Pb content is increased.

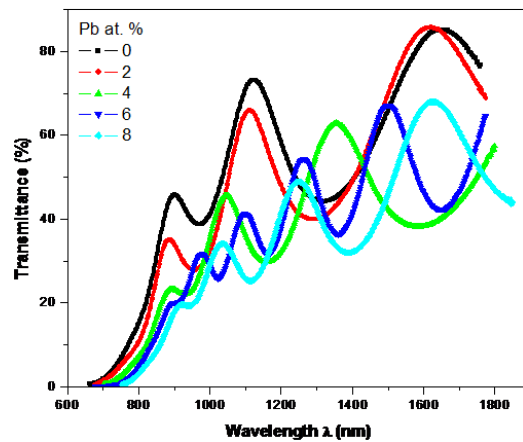


Fig. 2. Transmission spectra of as- prepared  $Se_{70-x}Te_{30}Pb_x$  thin films.

The spectral distribution of refractive index ( $n$ ) and extinction coefficient ( $k$ ) with wavelength is given in figs. 3 and 4 respectively. From the figs. 3 and 4 it is clear that both the refractive index and extinction coefficient decrease with the increase in the wavelength.

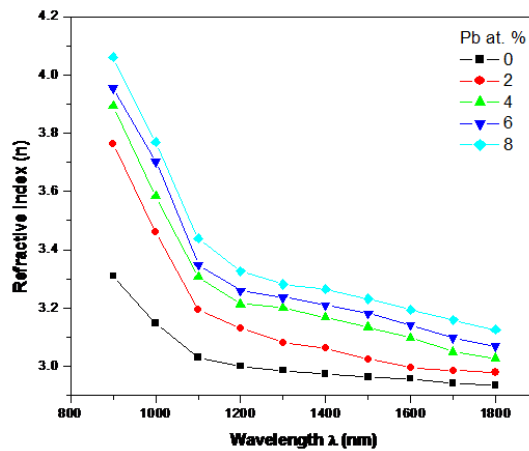


Fig. 3. Variation of refractive index ( $n$ ) with wavelength ( $\lambda$ ) in  $Se_{70-x}Te_{30}Pb_x$  thin films.

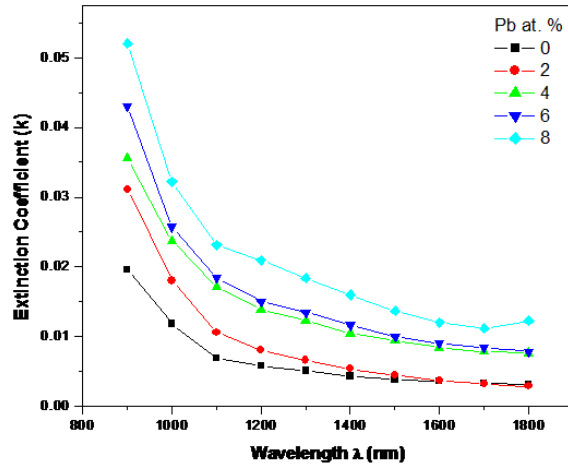


Fig. 4. Variation of extinction coefficient ( $k$ ) with wavelength ( $\lambda$ ) in  $Se_{70-x}Te_{30}Pb_x$  thin films.

### 3.2.2 Determination of dielectric constants

The real and imaginary dielectric constant of amorphous thin films has been calculated by the relation (9) and (10), respectively.

$$\varepsilon' = n^2 - k^2 \quad (9)$$

$$\varepsilon'' = 2nk \quad (10)$$

And dissipation factor,  $\tan \delta$ , is expressed as

$$\tan \delta = \frac{\varepsilon''}{\varepsilon'} \quad (11)$$

The variation of  $\varepsilon'$ ,  $\varepsilon''$  and  $\tan \delta$  with wavelength are shown in figure 5, 6, and 7 respectively. These are found to decrease with increase in wavelength.

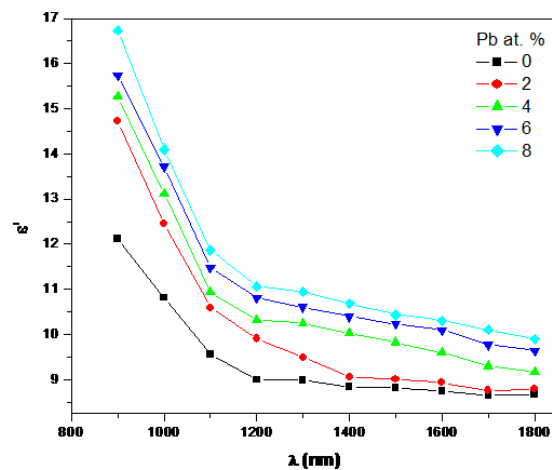


Fig. 5. Variation of real dielectric constant ( $\varepsilon'$ ) with wavelength ( $\lambda$ ) in  $Se_{70-x}Te_{30}Pb_x$  thin films.

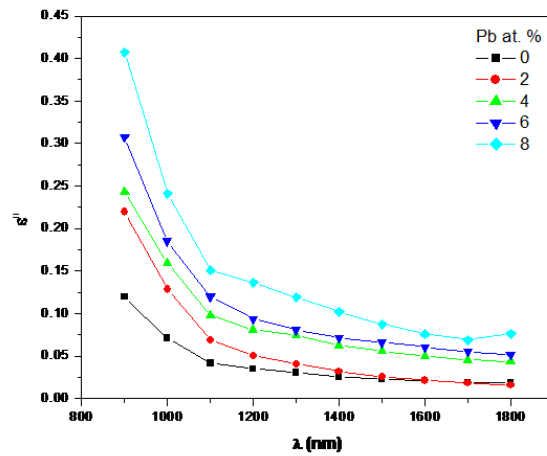


Fig. 6. Variation of imaginary dielectric constant ( $\epsilon''$ ) with wavelength ( $\lambda$ ) in  $Se_{70-x}Te_{30}Pb_x$  thin films.

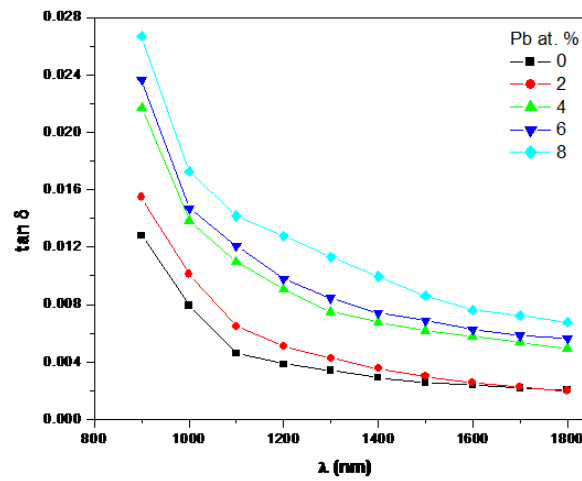


Fig. 7. Variation of dissipation factor ( $\tan \delta$ ) with wavelength ( $\lambda$ ) in  $Se_{70-x}Te_{30}Pb_x$  thin films.

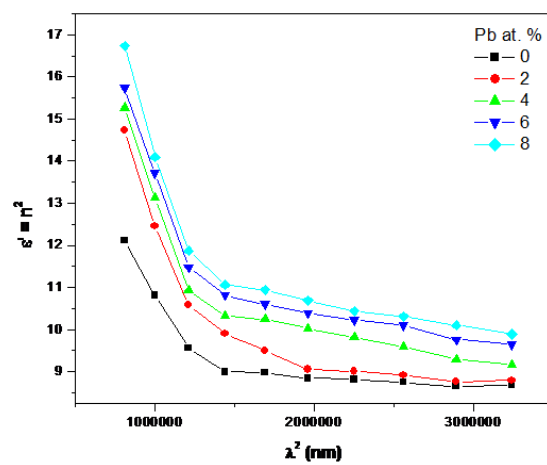


Fig. 8. Variation of real part of dielectric constant with square of wavelength in  $Se_{70-x}Te_{30}Pb_x$  thin films.

From Table 1, it is observed that the values of  $n \gg k$ . Therefore, assuming  $\epsilon' = n^2$ , the variation of  $\epsilon'$  with  $\lambda$  can be examined by using the eqn.

$$\epsilon' = n^2 = \epsilon_{\infty} - \left( \frac{e^2}{\pi c^2} \right) \left( \frac{n_c}{m^*} \right) \lambda^2 \quad (12)$$

Where  $\epsilon_{\infty}$  is lattice dielectric constant or (high frequency dielectric constant),  $e$  is the electronic charge,  $\frac{n_c}{m^*}$  is the ratio of free charge carrier concentration to the electron effective mass [15]. The obtained values of real part of dielectric constant  $\epsilon'$  are plotted as a function of  $\lambda^2$  as shown in fig. 8. The dependence of  $\epsilon'$  on  $\lambda^2$  is linear at longer wavelength. The intersection at  $\lambda^2 = 0$  for the linear part of the curve at higher wavelength gives the high frequency dielectric constant. It is also observed from the Table 1, that the  $\epsilon'$  and  $\epsilon_{\infty}$  increases with increase in Pb concentration.

### 3.3 Absorption coefficient and optical band gap

The spectral distribution of the absorption coefficient  $\alpha$  of the films was calculated from the equ. 8, using the calculated values of  $k$ . In the low absorption region, (where  $1 \text{ cm}^{-1} < \alpha < 10^4 \text{ cm}^{-1}$ ), is called Urbach's exponential tail region in which absorption takes place between valence band tail and conduction extended states and the absorption depends exponentially on the photon energy as given by the relation [16].

$$\ln(\alpha) = \ln(A) + \left( \frac{h\nu}{E_e} \right) \quad (13)$$

where  $A$  is a constant and  $E_e$  is interpreted as band tail width corresponding to the width of tails of localized states which generally represents the degree of disorder in an amorphous semiconductor [17]. The value of  $E_e$  is determined from the reciprocal of the slope of the relation between  $\ln\alpha$  and  $h\nu$ . A plot of  $\ln\alpha$  as a function of photon energy  $h\nu$  for  $\text{Se}_{70-x}\text{Te}_{30}\text{Pb}_x$  thin films is shown in fig. 9 and is found to increase with increase in photon energy.

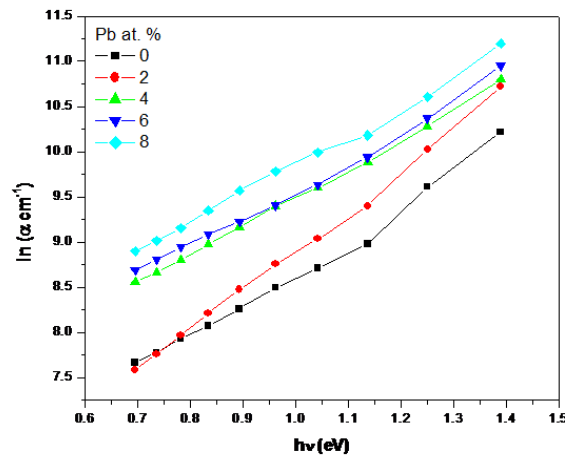


Fig. 9. Variation of  $\ln(\alpha)$  as a function of photon energy  $h\nu$ .

In the high absorption region (where  $\alpha > 10^4 \text{ cm}^{-1}$ ), the absorption takes place between valence and conduction band extended states and has the form (18)

$$\alpha h\nu = B (h\nu - E_g^{opt})^m \quad (14)$$

Where  $\alpha$  is the absorption coefficient;  $h\nu$  is the photon energy;  $B$  is the band tailing parameter that depends on the transition probability;  $E_g^{opt}$  optical energy gap;  $m$ -index, depending on the nature of electronic transitions. For amorphous materials non-direct optical transitions ( $m= 2$ ) are observed.

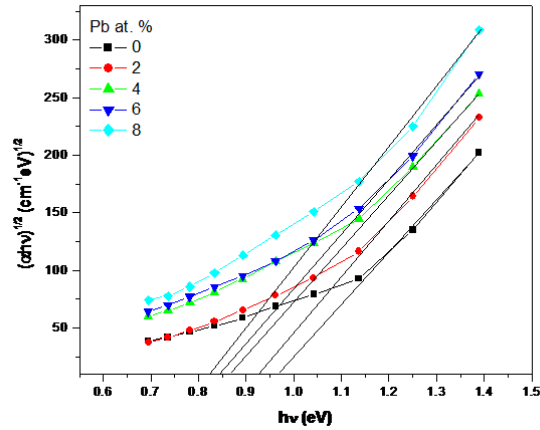


Fig. 10. Variation of  $(\alpha h\nu)^{1/2}$  as a function of photon energy  $h\nu$ , for  $Se_{70-x}Te_{30}Pb_x$  thin films.

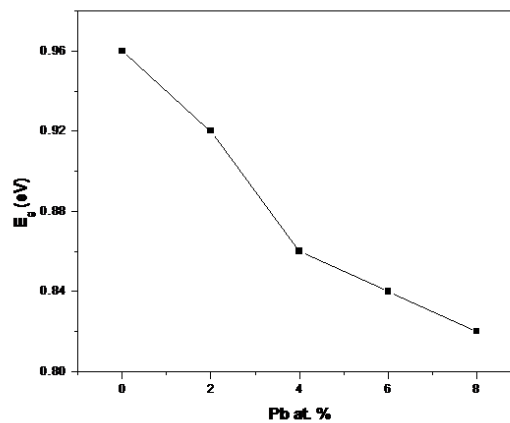


Fig. 11. Variation in band gap with Pb concentration.

The optical band gap  $E_g^{opt}$  can be determined by the extrapolation of the best fit line between  $(\alpha h\nu)^{1/2}$  and  $h\nu$  to intercept the  $h\nu$  axis for the  $Se_{70-x}Te_{30}Pb_x$  system as shown in fig. 10. The values of the optical band gap are plotted in fig. 11 as a function of Pb at. %. The calculated values of optical band gap of the  $Se_{70-x}Te_{30}Pb_x$  system are given in table 2. The value of band gap of system without lead is 0.96 eV. After incorporating Pb at. 2%, 4%, 6% and 8% in binary Se-Te alloy, it is observed that the optical band gap decreases from 0.92 eV to 0.82 eV.

Table 1. Values of refractive index ( $n$ ), extinction coefficient ( $k$ ), real part of dielectric constant ( $\epsilon'$ ), imaginary part of dielectric constant ( $\epsilon''$ ), dissipation factor ( $\tan \delta$ ), and high frequency dielectric constant ( $\epsilon_\infty$ ) of a  $Se_{70-x}Te_{30}Pb_x$  thin films at  $\lambda = 900$  nm .

Pb at. %	$n$	$K$	$\epsilon'$	$\epsilon''$	$\tan \delta$	$\epsilon_\infty$
0	3.3094	0.0195	12.121	0.1194	0.01280	9.24522
2	3.7632	0.0312	14.725	0.2191	0.01547	9.47255
4	3.8926	0.0356	15.269	0.2431	0.02171	10.99323
6	3.9538	0.0430	15.734	0.3077	0.02364	11.44784
8	4.0604	0.0521	16.738	0.4071	0.02669	11.90253

The decrease in optical band gap may be correlated with the electronegativity difference of the elements involved. The electronegativity of Se, Te and Pb are 2.4, 2.1 and 2.3 respectively and Pb has lower electronegativity than Se. The valance band in chalcogenide glasses is constituted by lone pair p-orbital's contributed by the chalcogen atoms. The substitution of electropositive element Pb for electronegative element Se may raise the energy of some lone pair states, which is further responsible for the broadening of the valance band inside the forbidden gap. This leads to band tailing and hence shrinking of the band gap. It is also evident from the table 2 that band tailing parameter increasing with increasing Pb content. Similar trend of optical band gap with increasing Pb content have been observed by P. Kumar Pal [19]

The optical band gap is a bond sensitive property [20]. Hence the change in the optical band gap, with Pb incorporation may also be understood on the basis of the change in the average bond energy of the system. The incorporation of Pb in  $\text{Se}_{70-x}\text{Te}_{30}\text{Pb}_x$  system resulting in the systematic replacement of Se-Te bonds (bond energy of 267.52 K J/mole) by Te-Pb bonds (bond energy of 252.0 K J/mole). Since Pb is added at the cost of Se which increases the probability for the formation of Te-Pb bonds. Since the energy of Te-Pb bond is lower than Se-Te bond, the average bond energy of the system decreases, results in the decrease in band gap.

### 3.4 Dispersion energy, oscillator strength, static refractive index from the Wemple-Didomenico model

Measured refractive indices were analyzed by using the Wemple model. According to a single-oscillator model (Wemple- DiDomenico model) [21, 22] the relation between the refractive index  $n$ , and photon energy  $h\nu$ , can be written as follows.

$$n^2(h\nu) = 1 + \frac{E_o E_d}{E_o^2 - (h\nu)^2} \quad (15)$$

Where  $h\nu$  is the photon energy,  $E_o$  is the oscillator energy and  $E_d$  is the oscillator strength or dispersion energy. The oscillator energy  $E_o$ , is an average energy gap, can be obtained by using eq. 15. Fig. 12 shows the plot of  $(n^2 - 1)^{-1}$  Vs  $(h\nu)^2$ , which is a straight line. The values of WDD dispersion parameters,  $E_o$  and  $E_d$ , for all the films, were determined directly from the slope  $(E_o E_d)^{-1}$ , and the intercept  $(E_o/E_d)$ , on the vertical axis. The values of the static refractive index  $n_0$ , for all the films were calculated from WDD dispersion parameters  $E_o$  and  $E_d$  by using a formula

$$n_0 = \left(1 + \frac{E_d}{E_o}\right)^{\frac{1}{2}} \quad (16)$$

The values of  $n_0$  are calculated by extrapolating the equation (15) towards  $h\nu = 0$  and the values of  $n_0$  are given in table 2.

From the figs. 11 and 12, the relationship  $E_o \approx 2E_g^{opt}$  is deduced, as it was found by Tanaka [23].  $E_o$ , is related to the average molar bond energy of the different bonds present in the system. Hence the decrease in  $E_o$  is a consequence of lower bond energy of Te-Pb bonds (252.0 K J/mole), when compared with that of the Se-Te bonds (267.52 K J/mole). Since Pb is added at the cost of Se which increases the probability for the formation of Te-Pb bonds. Since the energy of Te-Pb bond is lower than Se-Te bond, the average bond energy of the system decreases, results in the decrease in band gap. Furthermore,  $E_d$  obeys simple empirical expression [21, 22].

$$E_d = \beta N_c Z_a N_e \text{ (eV)} \quad (17)$$

Where  $\beta \approx 0.4$  eV, for covalent crystalline/ amorphous materials (&  $\beta \approx 0.3$  eV, for ionic materials),  $N_c$  is the coordination number of the cation nearest neighbour to the anion,  $Z_a$  is the formal chemical valency of the anion, and  $N_e$  is the total number of valence electrons.

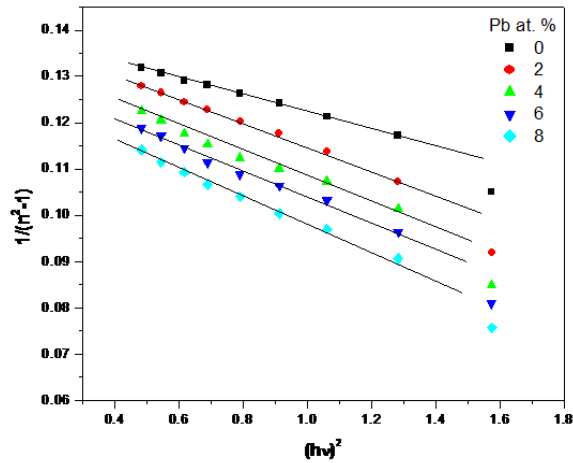


Fig. 12. Plot of the refractive index factor  $(n^2 - 1)^{-1}$  Vs  $(hv)^2$  of  $Se_{70-x}Te_{30}Pb_x$  thin films.

The calculated values of  $E_0$ ,  $E_d$ ,  $n_0$ , and  $E_g^{opt}$  are given in table 2. The explanation for the decrease in  $E_d$  and  $E_0$  may be given on the basis of increase in scattering centres due to incorporation of Pb atoms in the host glassy matrix.

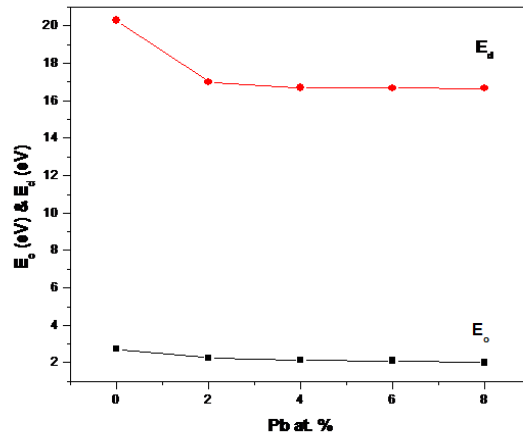


Fig. 13. Pb-content dependence of the single effective oscillator parameters  $E_0$  and  $E_d$ .

Table 2. Optical constants as a function of Pb- content of a  $Se_{70-x}Te_{30}Pb_x$  thin films.

Pb at. %	$E_g^{opt}$	$E_e$	$E_0$	$E_d$	$n_0$	$N_e$	$N_c$
0	0.96	0.325	2.74	20.29	2.89	8.5714	3.1982
2	0.92	0.341	2.26	17.01	2.92	8.7647	2.6219
4	0.86	0.355	2.14	16.70	2.97	8.9697	2.5164
6	0.84	0.364	2.10	16.68	2.99	9.1875	2.4534
8	0.82	0.372	2.00	16.65	3.06	9.4194	2.3887

#### 4. Conclusions

Thin films were prepared by thermal evaporation technique. The glassy nature of as deposited thin films is confirmed by X-ray diffraction analysis. The change in the optical band gap is explained on the basis of the average bond energy difference on addition of Pb atoms in Se-Te

system at the cost of Se. The oscillator energy  $E_0$  varied in proportion to  $E_g^{opt}$ , in accordance with the finding of Tanaka. The decrease in  $E_g^{opt}$ ,  $E_d$  and  $E_0$  is explained on the basis of electronegativity difference of constituent atoms and average bond energy difference of the system. On increasing Pb content the value of  $E_d$  decreases, owing to the decrease in the effective coordination number  $N_c$ .

### Acknowledgement

The authors would like to thank department of physics, Gurukula Kangri University, Haridwar for providing instrumental facilities sponsored by DST -FIST New Delhi (India).

### References

- [1] M. Kastner, Phys. Rev. Lett. **28** (6), 355 (1972).
- [2] J. A. Savage, Infrared Optical Materials and their Antireflection Coatings, Adam Hilger, Bristol (1985).
- [3] K. Shimakawa, Philos. Mag. **46**, 123 (1982).
- [4] S. O. Kasap, T. Wagner, V. Aiyah, O. Krylouk, A. Bekirov, L. Tichy, J. Mat. Sci. **34**, 3779 (1999).
- [8] Monisha Chakraborty, International Journal of Engineering Science and Technology **3**, 10 (2011).
- [9] R. Glang. Handbook of Thin Film Technology, Mc Graw- Hill, New York, (1983).
- [10] P. J. S. Ewen. A. Zakcry, A. P. Firth, A. E. Owen, Phil. Mag. B **57**, 1 (1988).
- [11] M. abkowitz, Polym. Engg.Sci. **24**, 1149 (1984).
- [12] R. Swanepoel, J. Phys. E: Sci. Instrum. **17**, 896 (1984).
- [13] R. Swanepoel, J. Phys. E **16**, 1224 (1983).
- [14] J. C. Manificier, J. Gasiot, J. P. Fillard, J. Phys. E: Sci. Instrum. **9**, 1002 (1976).
- [15] J. N. Zemel, J. D. Jensen, R. B. Schoolar, phys. Rev. A. **140**, 330 (1965).
- [16] M. M. Abdel – Aziz, E. G. El- Metwally, M. Fadel, H. H. Labib, M. A. Afifi, Thin Solid Films, **386**, 99 (2001).
- [17] J. A. Olley, Solid State Commun.,**13**, 1437 (1973).
- [18] J. Tauc, “Amorphous & Liquid Semiconductor”, New York: Plenum press (1974) p. 171.
- [19] P. Kumar Pal, H. Gupta, L. P. Purohit, K. Kumar, R. Kumar, R. M. Mehra, Journal of Ovonic Research, **10**, 127 (2014).
- [19] A. K. Pattanaik, A. Srinivasan, J. Optoelectron Adv. Mater. **5**, 1161(2003).
- [20] S. H. Wemple, M. DiDomenico, Phys. Rev. B. **3**, 1338 (1971).
- [21] S. H. Wemple, Phys. Rev. B. **7**, 3767 (1972).
- [22] K. Tanaka, Thin Solid Films **66**, 271 (1980).